Bull. Mater. Sci., Vol. 38, No. 5, September 2015, pp. 1449–1455. © Indian Academy of Sciences.

Electronic transport and magnetoresistivity of $La_{0.4}Bi_{0.1}Ca_{0.5-x}Sr_xMnO_3$ (x = 0.1 and 0.2)

P SUBHASHINI[1,*], B MUNIRATHINAM[2], M KRISHNAIAH[1], R VENKATESH[3], D VENKATESHWARLU[3] and V GANESAN[3]

[1]Department of Physics, Sri Venkateswara University, Tirupati 517 502, India
[2]NDT/SPP, SDSC, Sriharikota 524 124, India
[3]Low Temperature Laboratory, UGC-DAE Consortium for Scientific Research, University Campus, Khandwa Road, Indore 452 001, India

MS received 11 February 2015; accepted 10 April 2015

Abstract. Electrical resistivity and magnetoresistive behaviour of bismuth-substituted lanthanum manganites $La_{0.4}Bi_{0.1}Ca_{0.5-x}Sr_xMnO_3$ (x = 0.1 and 0.2) were systematically studied by varying the temperature from 2 to 300 K and the magnetic field up to 12 T. The samples were found to crystallize in rhombohedral structure and their morphology shows near-spherical nanosize crystallites. Charge ordering was observed in both the samples under zero field conditions and corresponding transition temperature T_{CO} was found to decrease with the increase of x. Resistivity measurements with magnetic field also showed suppression of magnetoresistivity (MR) with the increase of x and the maximum MR was found to be 98 and 93% for x = 0.1 and 0.2, respectively, at 10 T. In the high-temperature domain, the electronic transport was observed to be dominated by the variable range hopping mechanism for both the samples, whereas in the low-temperature domain the electrical conduction of x = 0.1 sample was observed to be contributed by various other electron scattering mechanisms.

Keywords. Manganites; X-ray diffraction; magnetoresistivity; charge ordering.

1. Introduction

Half-doped manganites $RE_{1-x}A_xMnO_3$ (x = 0.5; RE = La, Nd, Pr and A = Ca, Sr, Ba, Bi) have been studied extensively in recent years both experimentally and theoretically for their intriguing electric and magnetic properties.[1] One of the interesting features of these compounds (x = 0.5) is the co-existence of ferromagnetic (FM) and charge-ordered anti-ferromagnetic (AFM) phases in contrast to $0.15 < x < 0.5$, for which the ground state is FM metallic due to double exchange (DE) mechanism. The co-existence of these phases is usually explained in terms of close competition between them as a result of smaller energy difference between their ground states.[2] The type of ground state is sensitive to the average size $\langle r_A \rangle$ of A-site cation (La^{3+}, Si^{2+}, Ca^{2+} ions), hydrostatic pressure, magnetic field, chemical substitutions at the Mn site and the A-site ionic radii mismatch (σ^2).[3,4] Half-doped manganites in general show different types of ground states depending on the dominance of AFM and/or FM interactions and Jahn–Teller distortions.[5] However, the complex physics behind these is still to be fully understood and hence the need for further studies. It is known that the widely studied manganite $La_{0.5}Ca_{0.5}MnO_3$ ($\langle r_A \rangle$ = 1.198 Å) undergoes FM metallic (T_C ~ 225 K) and AFM insulating state (T_N ~ 150 K) with simultaneous ordering of orbital (Jahn–Teller), charge and spin (CE type).[6–8] The charge ordering (CO) of Mn^{3+} and Mn^{4+} ions below a temperature T_{CO} (~200 K) gives rise to the long-range localization of carriers to specific sites in the crystal. $La_{0.5}Sr_{0.5}MnO_3$ ($\langle r_A \rangle$ = 1.263 Å) on the other hand is found to be a FM metal (T_C ~ 310 K) with a weak A-type AFM ordering but no charge or orbital ordering.[9] $Nd_{0.5}Sr_{0.5}MnO_3$ ($\langle r_A \rangle$ = 1.236 Å) with T_{CO} ~ 158 K exhibits a CE-type AFM spin structure below 150 K and $Pr_{0.5}Sr_{0.5}MnO_3$ ($\langle r_A \rangle$ = 1.245 Å) reveals A-type spin structure below its ordering temperature.[10,11] Similar magnetic phases are found in $Pr_{0.5}Sr_{0.5-x}Ca_xMnO_3$ and $Pr_{0.5}Sr_{0.5-x}Ba_xMnO_3$ systems,[12–14] as a function of $\langle r_A \rangle$. The partial substitution of Nd^{3+} by La^{3+} ion in $(Nd_{1-z}La_z)_{0.5}Sr_{0.5}MnO_3$ results in the suppression of charge-ordered state and A-type AFM state is also found as an intermediate state as z is increased in this manganite system.[15] The above shows that change in $\langle r_A \rangle$ by substitution of cations of different sizes at rare earth ion sites causes lattice distortion and affects FM double exchange and AFM super-exchange interactions differently. In general, charge delocalized FM state is stabilized for large $\langle r_A \rangle$ and charge-ordered AFM insulating state is stabilized for small $\langle r_A \rangle$ at low

*Author for correspondence (subhashinisvu@gmail.com)

temperatures.[16] In other words, width of e_g electron bandwidth (W) favours FM double exchange interactions and narrow bandwidth favours an insulating state. It is to be noted that e_g electron bandwidth alone does not predict the occurrence of various magnetic phases in half-doped manganite systems: AFM ordering for instance is suppressed rather than enhanced in $La_{0.5-x}Y_xCa_{0.5}MnO_3$, where the substitution of Y decreases $\langle r_A \rangle$ but increases the disorder factor (σ^2).[17] σ^2 however is much reduced for the $La_{0.5}Ca_{0.5-x}Sr_xMnO_3$ series[18–20] and the same is selected for light doping with trivalent Bi^{3+} ions for La^{3+} ions. The substitution of Bi^{3+} does not introduce holes into the system and in fact makes the average size of MnO_6 octahedrons larger by about 0.5% larger than that with La^{3+} ions.[21] Recent studies of half-doped bismuth-substituted lanthanum manganites[22–24] show that the charge ordering behaviour is particularly sensitive to the local distortion caused by $6s^2$ lone pair of Bi^{3+} or to hybridization between Bi-6s orbitals and O-2p orbitals, which block the movement of e_g electrons through Mn–O–Mn bridges rather than to $\langle r_A \rangle$ as the ionic radius difference between Bi^{3+} (1.24 Å) and La^{3+} (1.22 Å) is negligibly small. For instance the CO temperature of $Bi_{0.5}Ca_{0.5}MnO_3$ is found to be relatively higher ($T_{CO} \sim 325$ K) as compared to $La_{0.5}Ca_{0.5}MnO_3$ and also exhibit C-type AFM structure in contrast.[22] In the present investigation, the Bi^{3+} percentage is kept constant while that of Sr^{2+} is varied at the expense of Ca^{2+} to study the CO behaviour as well as megneto-resistive characteristics.

2. Experimental

The polycrystalline samples of $La_{0.4}Bi_{0.1}Ca_{0.5-x}Sr_xMnO_3$ ($x = 0.1$ and 0.2) were synthesized using the low-temperature nitrate route method.[25] Briefly, 1 M solutions of 99% pure chemicals such as $La(NO_3)_3{\cdot}6H_2O$, $Bi(NO_3)_3{\cdot}5H_2O$, $Ca(NO_3)_2{\cdot}4H_2O$, $Sr(NO_3)_2$ and acetate such as $Mn(CH_3COO)_2{\cdot}4H_2O$ were used to prepare individually the solutions of specific molarity using distilled water. These solutions were mixed together using magnetic stirrer and slowly dried at 80°C. The resulting solid pulp was then calcined at 500°C for 7 h. The black powder thus obtained was ground thoroughly using a mortar and again was calcined at 900°C for 14 h. Finally around 1 g of each powder was pressed into pellet of 11 mm diameter and sintered at 900°C for another 14 h. X-ray diffraction patterns of both the samples were recorded using X-ray diffractometer (XRD) with CuKα radiation (λ = 1.5406 Å) in angular steps of 0.02°. The surface morphology was studied using scanning electron microscopy (SEM) and the compositions were verified by the energy-dispersive spectroscopy (EDS). The temperature-dependent electrical resistivity and magnetoresistivity of the samples were measured using Quantum designs made Physical Property Measurement System (PPMS). The temperature and magnetic field were varied in the range of 2–300 K and 0–12 T, respectively, during the measurements.

3. Results and discussion

3.1 *Crystal structure, composition and morphology*

The XRD patterns that are recorded in the angular range of 10–80° (figure 1) confirm that both the compounds exhibit rhombohedral structure with R3c space group. The lattice parameters are estimated using XRDA software with a maximum error of ± 0.009 Å (table 1).[26,27] The unit cell volume is observed to increase with the increase of x consistent with the fact that relatively bigger Sr^{2+} ions are substituted for Ca^{2+} ions.[19] The average crystallite size (d), as given in table 1, estimated using the Scherrer formula is found to be in the nanorange for both the compounds.

For the present samples σ^2 is however observed to be much reduced. The percentage of Bi^{3+} ions and hence the number of local distortions induced by the corresponding $6s^2$ lone pairs are kept constant for both the samples. The variation of $\langle r_A \rangle$ (table 1) is therefore expected to play a dominant role in affecting the overall structural, electrical and magnetoresistivity behaviour of these samples. The morphology of samples using SEM shows that the grains (~ 300 nm in diameter) are nearly spherical in shape and uniform in size (figure 2a and b). The elemental analysis of the samples confirms the presence of targeted elements and near-stoichiometric compositions (table 2).

3.2 *Electronic transport*

The electrical resistivity $\rho(T)$ of samples as a function of temperature is measured using the standard four-probe

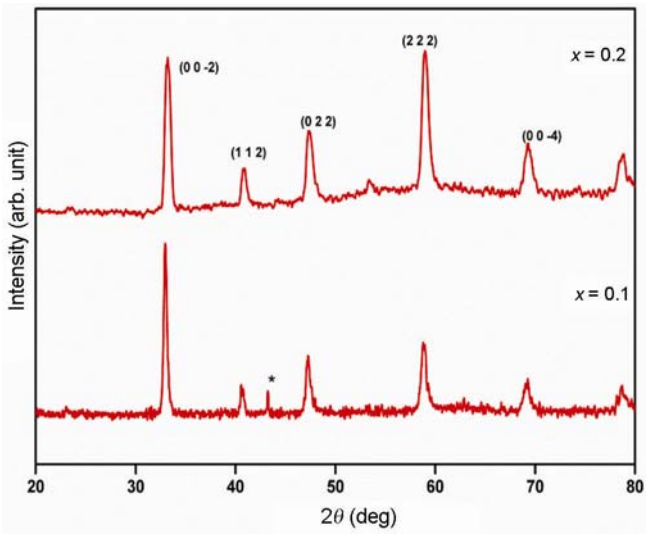

Figure 1. X-ray diffraction patterns of $La_{0.4}Bi_{0.1}Ca_{0.5-x}Sr_xMnO_3$ ($x = 0.1$ and 0.2).

Table 1. Structural parameters of $La_{0.4}Bi_{0.1}Ca_{0.5-x}Sr_xMnO_3$ ($x = 0.1$ and 0.2).

Compositions x	d (nm)	a (Å)	V (Å^3)	$\langle r_A \rangle$ (nm)	Tolerance factor (t)	σ^2 (nm^2) $\times 10^{-5}$
0.1	23	5.417	158.90	0.122	0.958	1.47
0.2	12	5.428	159.89	0.123	0.962	2.08

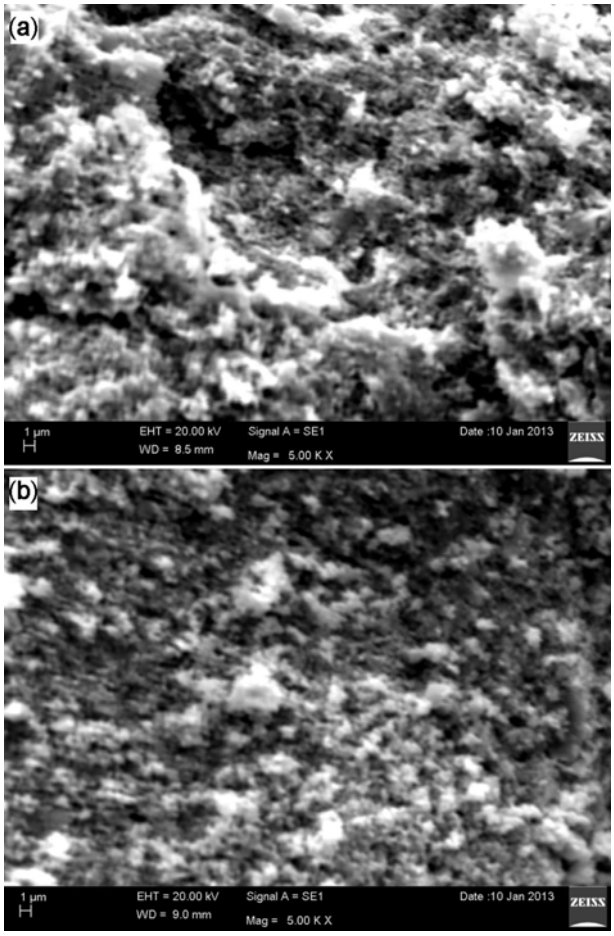

Figure 2. (**a** and **b**) SEM images of $La_{0.4}Bi_{0.1}Ca_{0.5-x}Sr_xMnO_3$ ($x = 0.1$ and 0.2).

Table 2. Atomic percentage of compounds obtained using EDS.

	Atomic percentage obtained (calculated) for $La_{0.4}Bi_{0.1}Ca_{0.5-x}Sr_xMnO_3$ samples	
Elements (%)	$x = 0.1$	$x = 0.2$
La	9.40 (8.0)	11.50 (8.0)
Bi	1.47 (2.00)	2.03 (2.0)
Ca	8.73 (8.00)	6.71 (6.00)
Sr	1.57 (2.00)	3.40 (4.00)
Mn	19.60 (20.0)	23.50 (20.0)
O	59.20 (60.0)	52.74 (60.00)

technique. The temperature of samples is varied from 2 to 300 K for resistivity measurement and the magnetic field is varied up to 12 T for magnetoresistivity measurements. The temperature-dependent resistivity of the samples during cooling phase is shown in figure 3. An insulator-to-metal

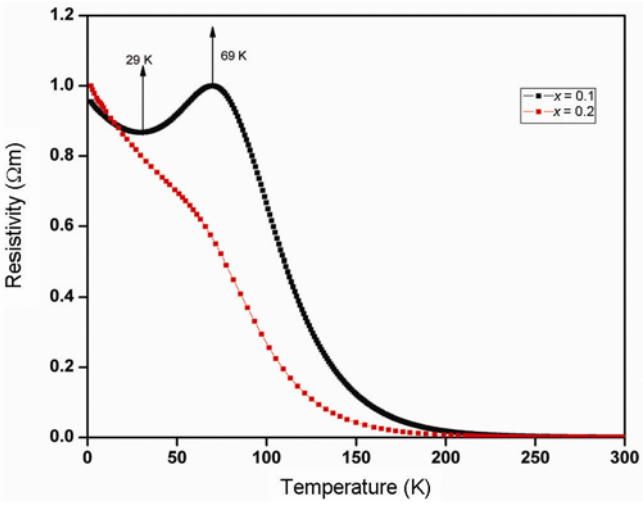

Figure 3. Temperature-dependent resistivity of $La_{0.4}Bi_{0.1}Ca_{0.5-x}Sr_xMnO_3$ ($x = 0.1$ and 0.2).

transition (T_{IM}) is observed for $x = 0.1$ sample at about 69 K, followed by metal-to-insulator transition (T_{MI}) at about 29 K. On the other hand, the resistivity of $x = 0.2$ sample exhibits semiconducting behaviour for the measured temperature range and also shows a relative fall when compared to that of $x = 0.1$ sample revealing relatively higher e_g electron bandwidth for the former. As the value of $\langle r_A \rangle$ is higher for $x = 0.2$ sample due to the substitution of larger ion (Sr^{2+}) for Ca^{2+} ion, the hopping amplitude of the itinerant e_g electron is expected to be relatively higher as the degree of overlap of Mn 3d and O 2p orbitals is sensitive to the variation of $\langle r_A \rangle$ and in fact increases as the value of $\langle r_A \rangle$ is increased.[28] Studies have shown that the increase of $\langle r_A \rangle$ increases Curie temperature (T_C)[29] and the tolerance factor also is found to have similar effect on the e_g bandwidth and T_C. Nine-fold coordination for A-site ions is assumed[30–33] for the calculation of both $\langle r_A \rangle$ and t-values (table 1).

The sharp increase in resistivity of both samples as the temperature is lowered from 300 K is attributed to the manifestation of charge ordering behaviour. The charge ordering transition temperature (T_{CO}) is found by locating the minimum of $d(\ln \rho)/dT$. The nature of these phase transitions of the samples is observed to be close to that of first order as the transitions are observed to be not completely reversible upon cooling and warming. Accordingly, T_{CO} of $x = 0.1$ sample is found to be 196 K for warming case and 190 K for cooling case and the same for $x = 0.2$ sample are found to be 157 K (warming) and 137 K (cooling). The decrease of T_{CO} with the

increase of x in the present samples is attributable mainly to the increasing percentage of Sr^{2+} ions at the expense of Ca^{2+} ions and the resulting larger $\langle r_A \rangle$ rather than to the special role of $6s^2$ lone pair of Bi^{3+} ions.

3.2a *High-temperature resistivity behaviour:* The electronic transport properties particularly in the paramagnetic phase of manganites are usually explained using different transport mechanisms: (i) a simple activation (SA) law, $\rho = \rho_0 \exp(E_a/k_B T)$, where E_a is the activation energy, (ii) adiabatic small polaron model (ASP), having its origin from the local lattice distortion accompanying the moving charge carrier (Jahn–Teller polaron) $\rho = AT \exp(E_a/k_B T)$, and the variable range hopping (VRH) model $[\rho = \rho_\infty [\exp(T_0/T)^{1/4}]]$, where ρ_∞ is the residual resistivity with the localization of charge carriers by the magnetic disorder,[26] where T_0 is the characteristic temperature. Accordingly, the resistivity behaviour of the present samples is investigated using the above models to determine the most probable mechanism of conduction in the high-temperature domain. Fitting of corresponding resistivity data of samples to the above models reveals that the VRH model is relatively better in simulating the transport behaviour of both the samples and negligible difference observed between the SA and ASP models comes in fitting the data (figure 4).

The VRH model gives a good fit in the temperature range from about 190 to 300 K for $x = 0.1$ sample and from about 150 to 300 K for the $x = 0.2$ sample as compared to small polaron model (180–300 K for $x = 0.1$ and 140–300 K for $x = 0.2$). The decrease in the value of characteristic temperature T_0 with the increase of x-value indicates decrease in bending of Mn–O–Mn bond or widening of e_g electron bandwidth.[34] The variation of carrier hopping energy (E_v), localization length ($1/\alpha$) and hopping distance (R) of the VRH model[26] reflect this behaviour of better conductivity with increase of x and $\langle r_A \rangle$, and similar is the variation of activation energy (E_a) of the SA and ASP models (table 3).

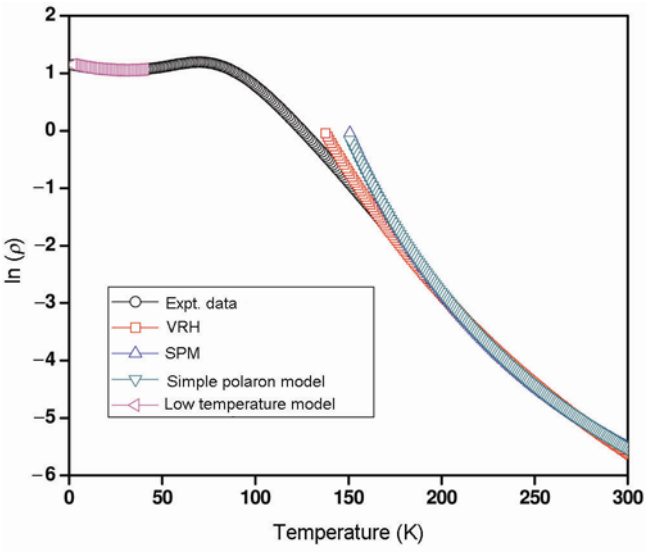

Figure 4. Fit of resistivity data to various transport models.

3.2b *Low-temperature resistivity behaviour:* In contrast to $x = 0.2$ sample in which the resistivity behaviour is observed to be semiconducting both below and above T_{CO}, the resistivity of $x = 0.1$ sample exhibits a local minimum at 29 K followed by sharp rise with further reduction of temperature. This kind of anomalous behaviour is observed to be similar to that reported for number of manganite compositions.[26,34,35] In this connection, various models involving the collective action of several different mechanisms are proposed to explain this low-temperature phenomenon.[26,36–39] Attempt to fit the resistivity data of $x = 0.1$ sample with the model $\rho(T) = a - b \ln T + cT^{1/2} + dT^2$ is found to be successful (figure 4). Apart from the usual Coulomb scattering term (dT^2), Kondo-like scattering ($b \ln T$) and correlated electron–electron interaction ($cT^{1/2}$) in weakly disordered system[40] figure in this model. Attempts to fit the low-temperature region resistivity data corresponding to the VRH, ASM and SA models are not successful.

3.3 *Temperature-dependent magnetoresistivity*

Figure 5a and b shows the variation of resistivity of $La_{0.4}Bi_{0.1}Ca_{0.5-x}Sr_xMnO_3$ ($x = 0.1$ and 0.2) samples for the entire temperature range of measurement as the magnetic field strength is varied from 0 to 12 T. The insulator-to-metal transition temperature of $x = 0.1$ sample is observed to shift to higher temperature range from 69 to 118 K as the magnetic field strength is increased from 0 to 12 T, indicating the suppression of charge-ordered insulating character. On the other hand, $x = 0.2$ sample although shows sharp fall in resistivity as the magnetic field is increased, it remains as a semiconductor even at 12 T.

Table 3. Fit parameters of electron transport models.

Electrical parameters	$x = 0.1$	$x = 0.2$
SA model		
ρ_0 (Ωm)	1.7293×10^{-5}	1.07×10^{-5}
E_a (eV)	0.14	0.11
ASP model		
A (Ωm K^{-1})	2.63×10^{-8}	3.04×10^{-8}
E_a (eV)	0.16	0.12
VRH model		
ρ_∞ (Ωm)	2.018×10^{-14}	1.52×10^{-12}
T_0 (K)	1.35×10^{8}	5.36×10^{7}
$1/\alpha$ (Å)	1.67	2.28
R (Å) at 300 K	16.24	17.6
E_v (eV) at 300 K	0.16	0.13

Defining the magnetoresistivity (MR) = $\{[\rho(T, H) - \rho(T, 0)]/\rho(T, 0)\} \times 100\%$, where $\rho(T, H)$ and $\rho(T, 0)$ are the resistivities measured with and without magnetic fields, respectively, MR behaviour of the samples is studied as a function of temperature at three different magnetic fields 1, 5 and 10 T (figure 6a and b).

Resistivity of $x = 0.1$ is found to be highly sensitive as compared to that of $x = 0.2$ sample for these magnetic field strengths. This behaviour is found to be in line with literature results,[21] wherein the MR is found to decrease with the increase of $\langle r_A \rangle$ and t. In addition, the MR is observed to flatten increasingly for both the samples as the magnetic field is increased and the temperature is lowered: the MR of $x = 0.1$ is found to be greater than 90% for the temperature range from 2 to 150 K, whereas the same for $x = 0.2$ is found to be in the range of 5–90 K. The MR is also observed to peak around 57 K for $x = 0.1$ (98%) and 54 K for $x = 0.2$ sample (94%). The high sensitivity of these compounds to external magnetic fields may be exploited for magnetic sensing applications.

The resistivity of the samples as a function of magnetic field is studied at selected temperatures. Figure 7a and b shows behaviour of magnetic field-dependent resistivity of $x = 0.1$ at $T = 30$, 70, 150 and 250 K and of $x = 0.2$ at $T = 60$, 140 and 250 K, respectively. Figure 7a reveals a relative drop in resistivity of 86% between 30 and 150 K for $x = 0.1$ sample under zero field conditions and thereafter it is found to decrease to a negligibly small value as the magnetic field increased to 12 T. Also the average rate of change of resistivity of $x = 0.1$ with field is found to be almost same at temperatures 30 and 70 K for magnetic field variation from 0 to 12 T, while the rate of reduction is almost negligible at 250 K. On the other hand, the drop in resistivity of $x = 0.2$ sample is found to

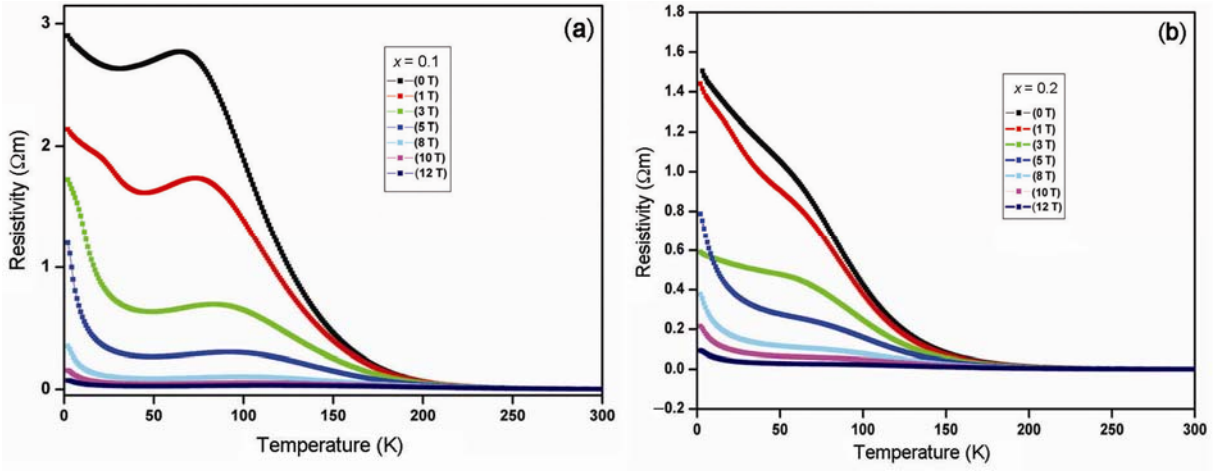

Figure 5. (**a** and **b**) Resistivity of $La_{0.4}Bi_{0.1}Ca_{0.5-x}Sr_xMnO_3$ as function of temperature and magnetic field.

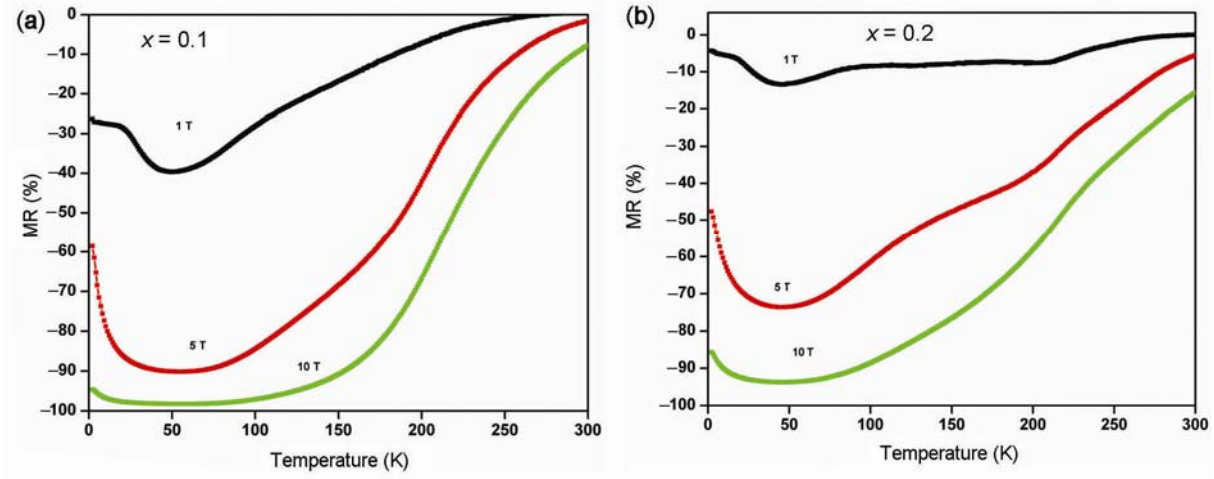

Figure 6. (**a** and **b**) Temperature-dependent magnetoresistivity of $La_{0.4}Bi_{0.1}Ca_{0.5-x}Sr_xMnO_3$.

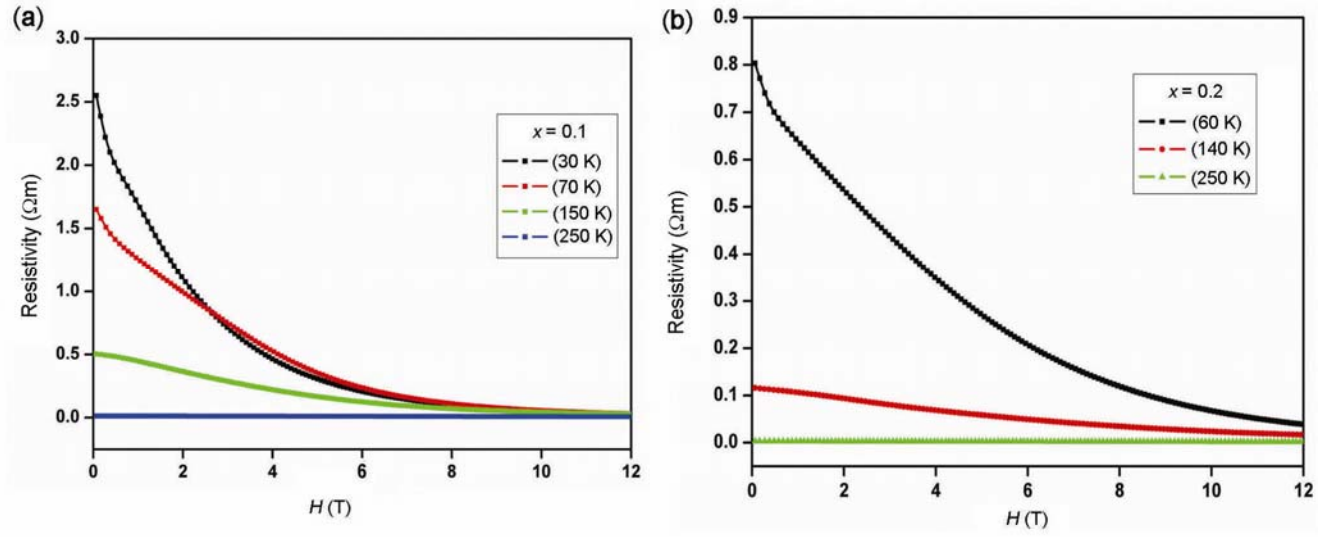

Figure 7. (**a** and **b**) Resistivity of $La_{0.4}Bi_{0.1}Ca_{0.5-x}Sr_xMnO_3$ as function of magnetic field.

be around 85% between $T = 60$ and 140 K at zero field conditions and the subsequent rate of decrease of resistivity with increase of magnetic field is however observed to be relatively smaller as compared to $x = 0.1$ sample.

4. Conclusion

Structural characterization, morphology, electronic transport and magnetoresistivity of $La_{0.4}Bi_{0.1}Ca_{0.5-x}Sr_xMnO_3$ ($x = 0.1$ and 0.2) are systematically investigated. Both the samples are found to crystallize in rhombohedral structures in contrast to orthorhombic structures, usually reported for lanthanum manganites and SEM of them shows nanosize spherical crystallites. The suppression of both charge ordering and magnetoresistivity with the increase of x is in line with that reported for bismuth-substituted half-doped manganites. The magnetoresistivity is observed to encompass the measured range of temperature as the magnetic field is increased. High sensitivity of resistivity of samples to the magnetic field with MR peaking close to 100% may be exploited for magnetic sensor applications. VRH mechanism is found to simulate the resistivity behaviour of both the samples in the high-temperature domain. The abnormal behaviour of resistivity of $x = 0.1$ sample in the low-temperature domain is observed to be contributed by a number of electron scattering mechanisms.

Acknowledgements

The first author would like to thank University Grant Commission (UGC) for providing Rajiv Gandhi National Fellowship to pursue doctoral degree research program at Sri Venkateswara University, Tirupati. Authors at Tirupati are thankful to UGC-DAE CSR, Indore, India, for providing MR facilities. DST, India, is acknowledged for their initial support in setting up the LTHM facilities at CSR, Indore.

References

1. Rao C N R, Arulraj A, Cheetham A K and Raveau B 2000 *J. Phys.: Condens. Matter* **12** 83
2. Levy P, Parisi F, Polla G, Vega D, Leyva G and Lanza H 2000 *Phys. Rev. B* **62** 6437
3. Attfield J P 1998 *Chem. Mater.* **10** 3239
4. Rodriguez-Martinez L M and Attfield J P 1998 *Phys. Rev. B* **58** 2426
5. Rao C N R and Raveau B 1998 *Colossal magnetoresistance, charge ordering and related properties of manganese oxides* (Singapore: World Scientific)
6. Radaelli P G, Cox D E, Marezio M and Cheong S-W 1997 *Phys. Rev. B* **55** 3015
7. Radaelli P G, Cox D E, Marezio M, Cheong S-W, Schiffer P E and Ramirez A P 1995 *Phys. Rev. Lett.* **75** 4488
8. Das A, Babu P D, Chatterjee S and Nigam A K 2004 *Phys. Rev. B* **70** 224404
9. Jirák Z, Hejtmánek J, Knížek K, Maryško M, Šima V and Sonntag R 2000 *J. Magn. Magn. Mater.* **217** 113
10. Kajimoto R, Yoshizawa H, Kawano H, Kuwahara H, Tokura Y, Ohoyama K and Ohashi M 1999 *Phys. Rev. B* **60** 9506
11. Kawano H, Kajimoto R, Yoshizawa H, Tomioka Y, Kuwahara H and Tokura Y 1997 *Phys. Rev. Lett.* **78** 4253
12. Damay F, Martin C, Maignan A, Hervieu M, Raveau B, Jirak Z, Andre G and Bouree F 1999 *Chem. Mater.* **11** 536
13. Krupicka S, Marysko M, Jirak Z and Hejtmanek J 1999 *J. Magn. Magn. Mater.* **206** 45
14. Autret C, Martin C, Hervieu M, Maignan A and Raveau B 2003 *Chem. Mater.* **15** 1886
15. Moritomo Y, Kuwahara H, Tomioka Y and Tokura Y 1997 *Phys. Rev. B* **55** 7549

16. Yu R C, Tang J, Yao L D, Matsushita A, Yu Y, Li F Y and Jin C Q 2005 *J. Appl. Phys.* **97** 083910
17. Babu P D, Das A and Paranjpe S K 2001 *Solid State Commun.* **118** 91
18. Sundaresan A, Paulose P L, Mallik R and Sampathkumaran E V 1998 *Phys. Rev. B* **57** 2690
19. Dhiman I, Das A, Mishra P and Panicker L 2008 *Phys. Rev. B* **77** 094440
20. Garcia-Munoz J L, Fronterea C, Aranda M A G, Llobet A and Ritter C 2001 *Phys. Rev. B* **63** 064415
21. Li R, Qu Z and Fang J 2011 *Physica B: Condens. Matter* **406** 1312
22. Xia Z C, Wu Y Y, Zhu G F, Hu A Z, Feng X N, Wang Y, Xiong C S, Yuan S L and Tang C Q 2008 *J. Magn. Magn. Mater.* **320** 368
23. Zhang R R, Kuang G L, Zhao B C and Sun Y P 2010 *Solid State Commun.* **150** 209
24. Ahmed A M 2004 *Physica B* **352** 330
25. Pai M R, Wani B N and Bharadwaj S R 2006 *J. Indian Chem. Soc.* **83** 336
26. Munirathinam B, Krishnaiah M, Devarajan U, Esakki Muthu S and Arumugam S 2012 *J. Phys. Chem. Solids* **73** 925
27. Desgreniers S and Lagarec K 1998 *J. Appl. Crystallogr.* **31** 109
28. Neumeier J J, Hundley M F, Thompson J D and Heffner R H 1995 *Phys. Rev. B* **52** 7006
29. Hwang H Y, Cheong S W, Radaelli P G, Marezio M and Batlogg B 1995 *Phys. Rev. Lett.* **75** 914
30. Shannon R D 1976 *Acta Crystallogr. Section A* **32** 751
31. Wang X, Pan I Y W, Cui Q L, Zhang J, Gao W and Zou G T 2001 *J. Solid State Chem.* **160** 307
32. Zhao Y D, Jonghyurk Park, Jung R J, Noh H J and Oh S J 2004 *J. Magn. Magn. Mater.* **280** 404
33. Cheng Z X, Silver T M, Li A H, Wang X L and Kimura H 2004 *J. Magn. Magn. Mater.* **283** 143
34. Venkataiah G and Venugopal Reddy P 2005 *Solid State Commun.* **136** 114
35. Rozenberg E, Auslender M, Felner I and Gorodetsky G 2000 *J. Appl. Phys.* **88** 2578
36. Auslender M, Kar'kin A E, Rozenberg E and Gorodetsky G 2001 *J. Appl. Phys.* **89** 6639
37. Sarkar T, Ghosh B, Chatterji T and Raychaudhuri A K 2008 *Phys. Rev. B* **77** 235112
38. Lalitha G and Venugopal Reddy P 2010 *J. Alloys Compd.* **494** 476
39. Pekala M, Drozd V, Fagnard J F, Vanderbemden Ph and Ausloos M 2009 *J. Appl. Phys.* **105** 013923
40. Lee P A and Ramakrishnan T V 1985 *Rev. Mod. Phys.* **57** 287